Int. J. Electrochem. Sci., 9 **(2014)** 6020 - 6032

International Journal of
ELECTROCHEMICAL
SCIENCE
www.electrochemsci.org

Study of Bi film Formation on Different Carbon Based Electrodes for Possible Applicability in Electroanalytical Determination of Cysteine

Nives Vladislavić, Slobodan Brinić[*]*, Zoran Grubač, Marijo Buzuk*

Department of Chemistry, Faculty of Chemistry and Technology, University of Split, Teslina 10/V, 21000 Split, Croatia
[*]E-mail: brinic@ktf-split.hr.

Received: 10 June 2014 / *Accepted:* 27 June 2014 / *Published:* 25 August 2014

The bismuth film formation from acid nitrate solution on glassy carbon electrode (GCE), graphite electrode (GPE) and on an assembly of carbon fiber microelectrodes (CFME) were studied utilizing cyclic voltammetry (CV) and chronoamperometry (CA). Voltamemetric data obtained with all three electrodes indicate that bismuth electrodeposition is controlled by diffusion of Bi^{3+}. In the case of GCE and GPE Bi^{3+} diffusion coefficient was calculated using Randles-Sevcik equation. Analysis of the experimental current transients, obtained with GCE and GPE, revealed that increment of Bi^{3+} concentration changes nucleation mechanism from three-dimensional (3D) progressive nucleation toward instantaneous. Transients obtained with CFME, at different Bi^{3+} concentrations, suggesting only 3D instantaneous nucleation mechanism. Obtained data were used for preparation of appropriate Bi layer on CFME (Bi-film/CFME) for electroanalytical determination of cysteine by using square wave cathodic stripping voltammetry (SWCSV). Optimization of the SWCSV parameters have resulted in good linearity over examined concentration range of 1.0 μmol dm^{-3} to 10.0 μmol dm^{-3}, with detection limit of 0.028 μmol dm^{-3} and sensitivity of 398 nA μmol^{-1} dm^3.

Keywords: bismuth film, nucleation, carbon electrodes, stripping voltammetry, cysteine

1. INTRODUCTION

When general trend for more environmentally friendly analytical methods get in focus, bismuth film electrodes (BiFE) were proposed in advanced electroanalysis as an alternative to traditionally used mercury film electrodes. BiFE electrodes may be prepared by electrodeposition of thin bismuth film onto different metal substrates as Au [1], Cu [2], or Pt [3], but the most frequently used substrates have been carbon-containing materials. Recently, a few excellent review papers [4, 5, 6] about these types of electrodes, as well as the generally [3, 7, 8] or more specific [9, 10] reviews about bismuth

electrodes in electroanalysis, were published These papers contain a detail information about modifiers, electrode modification methods, advantage of some specific modification, detection techniques and limits of detection (if electrode was used in analytical determination).

Although Wang et. al [11] reported that the bismuth-coated glassy carbon and bismuth-coated carbon fiber electrodes display relatively similar signal-to-background characteristics despite different surface morphologies (bismuth-coated glassy carbon electrode indicates a highly porous, three-dimensional fibril-like network, while a thick, quite uniform, nonporous bismuth deposit was observed on the carbon fiber substrate), some advantages of the carbon fiber over glassy carbon such as decreasing of capacitive current, increasing of mass transfer rate, faster equilibrium time and negligibly ohmic drop were noticed [5]. Although the resistance of microelectrode is much higher than macroelectrode, carbon fiber electrodes (as kind of microelectrodes) exhibit steady state current densities that are easy to analyze and interpret, thus most its applications are in analytical or mechanistic studies [12]. The same observations are valid for the case of the random assemblies of microelectrodes [13].

Thus, it is very important to get insight into the type of nucleation and into the growth mechanism of bismuth on these substrates, in order to obtain bismuth deposits with desirable properties. The study of nucleation mechanism via electrochemical methods offer some advantages over other methods, as the driving force of the nucleation can be controlled by changing electrochemical parameters. The mechanism of nucleation includes instantaneous and progressive nucleation and the direction of nucleation includes two-dimensional (2D) and three-dimensional (3D) growth. Many parameters, such as: mass transport of bismuth species, deposition potential, temperature, nature of substrate, pH, concentration of bismuth species in solution, etc. influences on the nucleation and growth involve. When the rate of process is limited by mass transport in the solution, resulting current can be represented by Cottrell equation, while mechanism of nucleation can be described by Scharifker-Hills models [14].

Based on previously published papers [15, 16] that investigated electrocrystallization of copper and nickel on random assembly carbon microelectrode, the aim of this work has been to verify possibility and criteria of bismuth film formation on various type of carbon based electrodes. Electrochemical technique such as cyclic voltammetry (CV) and chronoamperometry (CA) were used for studying the nucleation and growth process. Analysis of obtained data by appropriate theoretical model can reveal the mechanism and parameters under which bismuth deposition occurs. Furthermore, this information has been used in preparation of appropriate Bi-film for applicability in electroanalytical determination of cysteine.

2. EXPERIMENTAL

2.1. Chemicals and solutions

Carbon fibers were obtained from Good-fellow (LS 249697; filament diameter 7μm; 36000 fibers) while sample of glassy carbon Sigradur was supplied by Hochtemperatur-Werkstoffe GmbH,

Germany. The pyrolytic graphite was obtained from GE Advanced Ceramics. All solutions were prepared from analytical grade chemicals. Potassium ferrocyanide ($K_4[Fe(CN)_6]$) was obtained from Merck. Nitric acid, sodium acetate, sodium chloride and acetic acid, all purchased from Kemika, Zagreb, were prepared by dissolution in redistilled water. Stock solution of the bismuth nitrate (20.0×10^{-3} mol dm^{-3}) was prepared by dissolution of $Bi(NO_3)_3 \times 5H_2O$ (99.99 %), obtained from Sigma-Aldrich, Inc., USA, in 0.5 mol dm^{-3} HNO_3. Lower concentrations of Bi^{3+} were prepared by dilution of the stock solution, by adding 0.5 mol dm^{-3} HNO_3. Solution of L-cysteine (from Merck) was prepared daily by dissolution of appropriate amount of the amino acid in redistilled water, previously deaerated with N_2.

2.2. Electrodes fabrication and bismuth film deposition

Carbon fiber microelectrodes (CFME) were fabricated by dip-coating of carbon fibers in epoxy resin. Glassy carbon electrode (GCE) was fabricated by encapsuling a glassy carbon rod (diameter 6 mm) into epoxy resin. Graphite electrode (GPE, diameter 6 mm) was prepared in same manner as GCE.

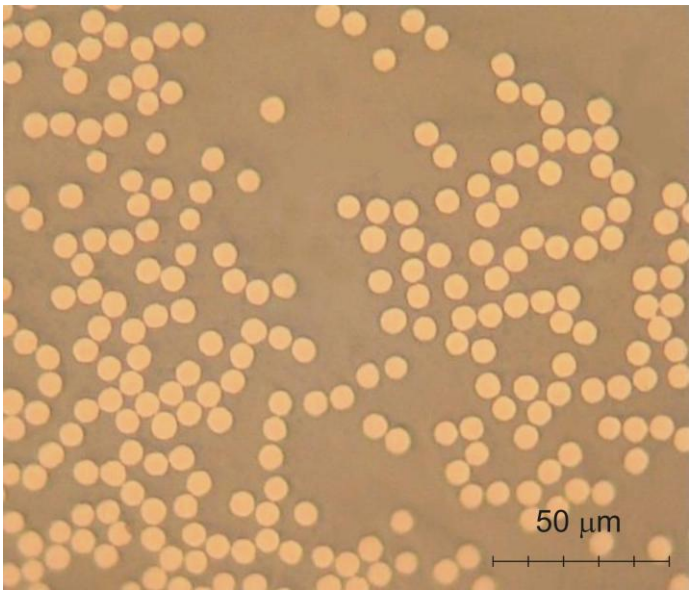

Figure 1. Micrograph of a random array CFME obtained using metallographic microscope. Each microelectrode consists of well-defined a disc-shaped carbon fiber.

The resulting CFME was inspected optically using an inverted microscope (Fig. 1). The real surface of the CFME, GCE and GPE were derived by CV in a solution containing 2.55×10^{-3} mol dm^{-3} of ferrocyanide in a 1.8 mol dm^{-3} NaCl according [17]. The obtained value was 0.014 cm^2, 0.283 cm^2 and 0.398 cm^2 respectively.

Before use, all electrodes, which served as substrate electrodes in all experiments, were mechanically polished with emery paper (2000 grit) followed by polishing with alumina powder down

to 0.05 μm. After polishing, electrodes were treated ultrasonically in redistilled water, rinsed with ethanol and finally rinsed with redistilled water. All experiments were carried out at 25 ºC in a three electrode cell, with CFME, GCE or GPE as working, and platinum as counter electrodes. Saturated calomel electrode (SCE) was used as reference electrode, to which all the measured potentials were referred. In order to achieve a reproducible and active electrode surface, the electrodes were repetitive cyclized (50 cycles) in 0.5 mol dm^{-3} HNO_3, over potential range -1.0 V to 1.0 V (scan rate of 100 mV s^{-1}). Prior cyclization electrodes were first kept at -1.2 V for 60 s, than at +1.5 V for 60 s [18].

Bismuth film formation was studied by CV and CA in 0.5 mol dm^{-3} HNO_3 with different Bi^{3+} concentration (20.0, 10.0, 5.0, 1.0, 0.5 × 10^{-3} mol dm^{-3} and additionally 0.1 and 0.05 × 10^{-3} mol dm^{-3} for CFME). In order to clean the electrode surface, before each measurements, electrodes were polarized at +0.7 V for 60 s.

Cyclic voltammograms were recorded, going from 0.0 V to the cathodic direction, reversed at -0.3 V, than reversed at +0.5 V and ended at 0.0 V. Chronamperometric experiments were carried out by applying a cathodic pulse from +0.3 V to different formation potential.

2.3. Cysteine determination

For electroanalytical determination of the cysteine, CFME was used. After addition of appropriate amount of cysteine the accumulation was performed at cathodic potential (-0.4 V) during 540 s in stirred solution and 60 s in quiescent solution. A square wave cathodic stripping voltammetry (SWCSV) was performed in quiescent solutions from -0.4 V toward -0.8 V, with potential scan frequency of the 50 Hz, pulse height of the 50 mV and potential increment of the 5 mV. Before determination, a background response was recorded at same condition as mentioned above. These measurements were carried out in deaerated solutions and nitrogen blanket was kept above solution during cysteine determination.

2.4. Apparatus

Electrochemical measurements were carried out with an Autolab PGSTAT 302N modular electrochemical system (Eco Chemie Ultecht, The Nederland), connected to PC and driven by GPES 4.9 Software (Eco Chemie) and NOVA 1.2 (Eco Chemie). All experiments were carried out at 25 ºC controlled by Huber CC1 (Offenburg, Germany) thermostat.

3. RESULTS AND DISCUSSION

3.1. Cyclic voltammetry

Definition of the potential region for bismuth deposition and dissolution on different carbon based electrodes were determined by cyclic voltammetry.

The cyclic voltammograms obtained at GPE and CFME electrodes in the presence of different concentration of Bi^{3+} in a nitrate solution are presented in Figure 2. Figure 3 shows cyclic voltammograms recorded at GCE as dependent on the potential scan rate. The obtained voltammograms revealed well-defined cathodic and anodic peaks, which correspond to bismuth deposition and dissolution.

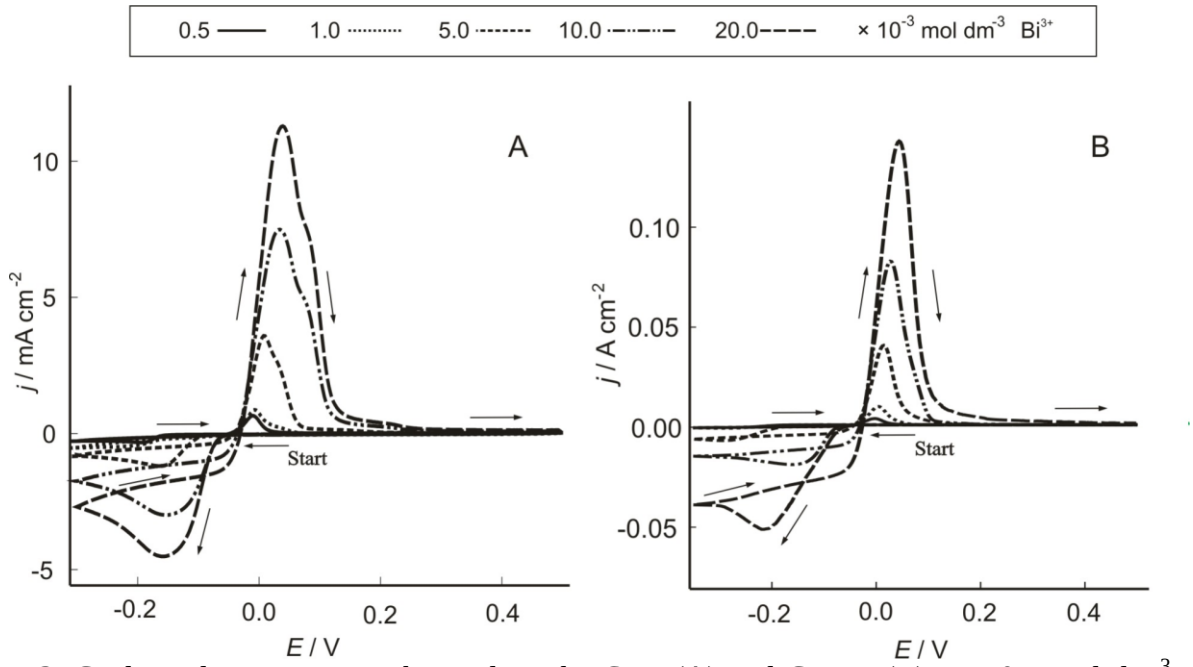

Figure 2. Cyclic voltammograms obtained on the GPE (A) and CFME (B) in a 0.5 mol dm^{-3} HNO_3 solution containing 0.5, 1.0, 5.0, 10.0 and 20.0 × 10^{-3} mol dm^{-3} Bi^{3+} , with scan rate of 20 mV/s, going from 0.0 V to the cathodic direction, reversed at -0.3 V, than reversed at +0.5 V and ended at 0.0 V.

From the voltammograms it can be seen that the bismuth deposition potential has more negative value than its Bi^{3+}/Bi equilibrium potential. By decreasing of Bi^{3+} concentration and upon increasing of the scan rate deposition, cathodic peak potentials become more negative, indicating insufficiently fast kinetics of bismuth nucleation. This behavior was noticed for all three types of electrodes.

Similar behavior can be found in related papers [19, 20, 21], where higher deposition potential of metallic ions on a foreign substrate was explained by nucleation overvoltage due to crystallographic substrate-metal misfit. However, in anodic direction the oxidation potential is close to the metal/metal ion equilibrium potential, as oxidation of metal starts from the surface with deposited metal [22]. Thus, the presence of the crossover on voltammograms may be reliable diagnostic tool for the formation of bismuth nuclei on foreign substrates.

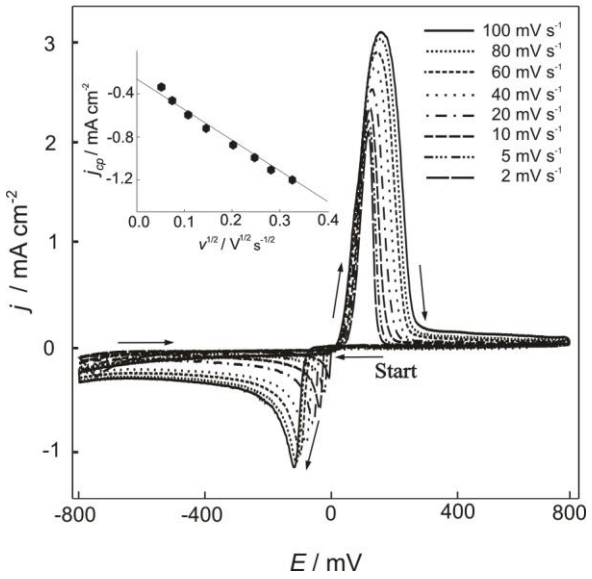

Figure 3. The influence of the potential scan rate (v) on cyclic voltammograms recorded on the GCE in a 0.5 mol dm^{-3} HNO_3 solution containing 1.0 × 10^{-3} mol dm^{-3} Bi^{3+}; v = 2, 5, 10, 20, 40, 60, 80 and 100 mV s^{-1}. *The inset*: dependence of the cathodic peak current density (j_{cp}) on the square root of the scan rate ($v^{1/2}$).

Linear relationship, obtained on inset of the Figure 3, between cathodic peak current density (j_{cp}) and the square root of scan rate (equation 1) indicates that the deposition process is limited by Bi^{3+} diffusion from bulk solution. Diffusion coefficient can be calculated by using Randles – Sevcik equation (1):

$$j_{cp} = 2.69\times10^5 z^{3/2} v^{1/2} D^{1/2} c \qquad (1)$$

where j_{cp} is the cathodic peak current density (A cm^{-2}), z is the total number of electrons, c is the bulk concentration of reactant species (mol cm^{-3}), D is the diffusion coefficient of reactant species (cm^2 s^{-1}), v is the scan rate (V s^{-1}),

Calculated coefficient for diffusion of Bi^{3+} to GCE from the solution containing 1.0 × 10^{-3} mol dm^{-3} Bi^{3+} was 5.8 × 10^{-6} cm^2 s^{-1}. Same method was used for determination Bi^{3+} diffusion coefficient in the case of GPE and CFME electrode and obtained value was 7.3 × 10^{-6} cm^2 s^{-1} and 163.0 × 10^{-6} cm^2 s^{-1}, respectively. As it can be seen, values for GCE and GPE are close to those reported for linear diffusion at a planar electrode [21].

However, the high value of the diffusion coefficient calculated from data obtained at CFME by Eqs. 1 indicates inadequacy of this method when CFME serves as working electrode. An important consequence of CFME geometry is that the current density is not uniform across the face of the inlaid micro fiber, but is greater at the edge. Thus the flux towards the nuclei located near the edge of an inlaid micro fiber is larger than the flux to the nuclei located far away from the electrode edge [23], which can be the reason why higher values for D have been obtained from CV measurements on CFME. When diffusion fields grow to a size much larger than micro fibers radii, r, the separated diffusion fields merge into a single larger field, exhibiting linear diffusion [24]. Then the steady state will be reached and the steady state current density (j_{ss}) can be expressed as [25]:

$j_{ss} = 4\ n\ z\ F\ D\ c\ r\ /\ A$ (2)

where F is Faraday constant, n number of microfibers and A is the area of the electrode (cm^2).

From value of steady state current density, established during CA measurements with CFME, calculated Bi^{3+} diffusion coefficient according to expression (2), was 1.4×10^{-6} cm^2 s^{-1}.

3.2. Chronoamperometry

The initial stage of bismuth electrodeposition was studied using potentiostatic pulse technique – chronoamperometric method. The potentiostatic pulses were applied from + 0.3 V to the various potentials in the range of bismuth nucleation and growth.

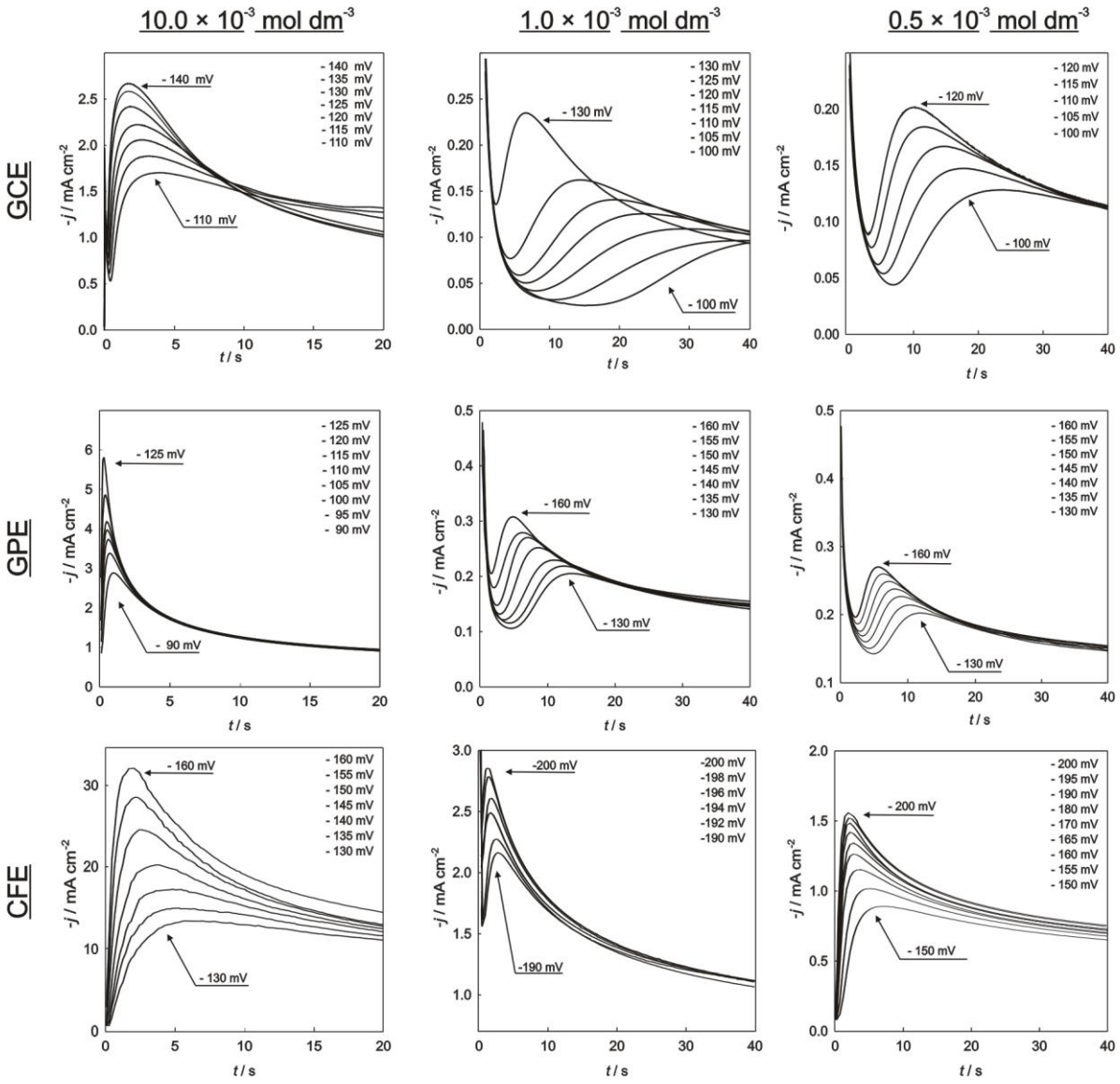

Figure 4. Current–time (potentiostatic) transients for the nucleation and growth of bismuth on the GCE, GPE and CFME recorded at various formation potentials, E_f, in a 0.5 mol dm^{-3} HNO_3 solution with different Bi^{3+} concentration.

The sets of current transients for the nucleation and growth of bismuth on different electrodes, obtained at the selected potentials in the solutions with various concentration of Bi^{3+}, are shown in Figure 4. The shape obtained is typical for the nucleation and growth of deposits on a conducting surface. As the transient potential (E_t) shifts to the cathodic side, the current maximum (j_m) increases, while the corresponding time (t_m) decreases. Following decay of charging current, the portion of current increase is determined by the nucleation mechanism, while the current decrease at long times ($t > t_m$) follows the Cottrell behavior [26].

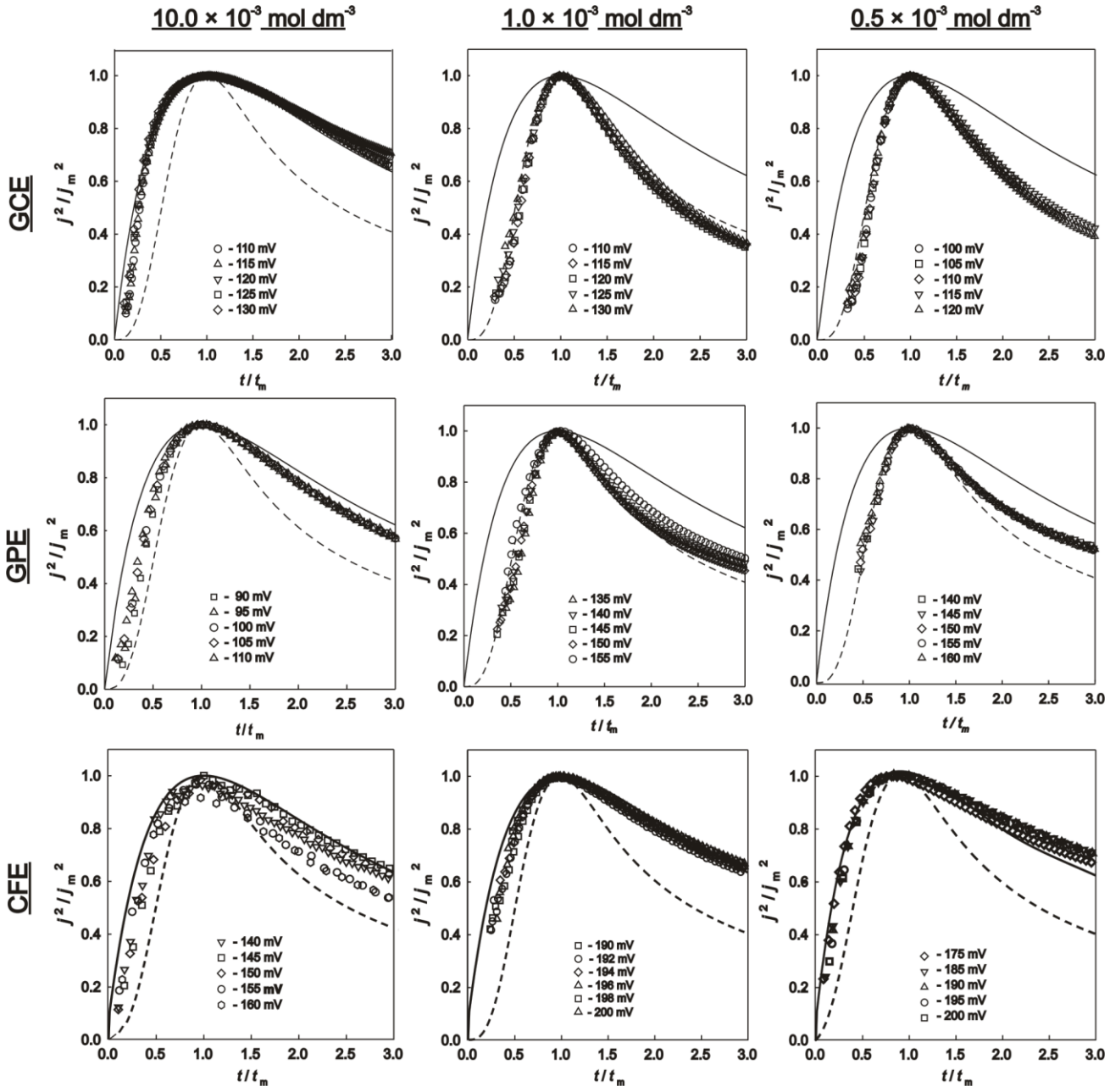

Figure 5. Normalized potentiostatic transients from Figure 4. The symbols are experimental values and the lines represent theoretical curves for the 3D instantaneous (solid line) and progressive (dashed line) type of nucleation and growth under diffusion control.

This suggests that qualitative analysis can be done using Scharifker - Hills models [27] for 3D nucleation and under the diffusion control. According to this model, there are two limiting nucleation mechanisms, the instantaneous and progressive. Instantaneous nucleation corresponds to a growth of nuclei on the active sites activated simultaneously. Progressive nucleation corresponds to a growth of nuclei on those active sites which are activated during the course of electroreduction [28].

The expressions for instantaneous and progressive nucleation with 3D growth are given by Eqs. (3) and (4), respectively,

$$\frac{j^2}{j_m^2} = \frac{1.9542}{t/t_m}\left\{1-\exp\left[-1.2564(t/t_m)\right]\right\}^2 \qquad (3)$$

$$\frac{j^2}{j_m^2} = \frac{1.2254}{t/t_m}\left\{1-\exp\left[-2.3367(t/t_m)^2\right]\right\}^2 \qquad (4)$$

where j_m and t_m are the current density and time coordinates of the chronoamperometric peak.

According to the model, nuclei population density can be calculated for different bismuth concentrations as a function of peak current density j_m and corresponding peak time, t_m.

Non-dimensional j^2/j^2_m vs. t/t_m plots of the experimental data presented in Figure 4, are shown in Figure 5 together with the theoretical curves for 3D instantaneous (the full line) and progressive nucleation (dashed line) and growth under diffusion control.

The plots obtained for GCE and GPE clearly suggests that bismuth nucleation and growth mechanism is highly influenced with Bi^{3+} concentration. By increasing Bi^{3+} concentration, the nucleation mechanism changes from 3D progressive toward 3D instantaneous, thus suggesting facilitation formation of dense and uniform deposits at higher bismuth concentration. The positive effect of metal ion concentration on the nuclei density was also observed by Grujcic and Pesic [29] and by Yang and Hu [20], which was explained by competition between the nucleation and grow. At an electrode surface metal atoms have two ways to reside: incorporating to existed nuclei or forming new nuclei. At higher concentration of metal ions the formation of new nuclei will be preponderant for the systems where the metal-substrate interaction energy is bigger than the metal-metal interaction energy. Nucleation and growth mechanism on GCE and on GPE showed no significant dependence upon applied potential in measured concentration range.

Contrary to transients obtained on GCE and on GPE, Fig. 5 reveals that type of 3D nucleation and growth of bismuth on CFME is not dependent on the Bi^{3+} concentration. The transients obtained in the concentrations range from 0.05 mM (not shown) to 10 mM, suggest on 3D instantaneous nucleation and growth. This may be attributed to an active surface segmentation of CFME rather than to large interaction energy between active surface and bismuth metal.

3.3. Applicability of Bi-film/CFME in electroanalytical determination of cystein

Cysteine plays an important role in biochemical processes and environmental systems [30, 31] and its determination has attracted considerable attention up to nowadays. In this sense,

electrochemical methods present advantages of simplicity and high sensitivity.

For the determination of cysteine, square wave cathodic stripping voltammetry (SWCSV) on previously accumulated bismuth(III) cysteinate at Bi-film/CFME, was applied. This can be done according to electroreduction reaction [32, 33]

$Bi(CyS)_3$ (ads) + $3e^-$ → Bi (s) + $3CyS^-$ (5)

Proposal for the formation of a bismuth(III) cysteinate surface species is based on the existence of mercury cysteinate surface species on Hg electrodes [34, 35], identification of various bismuth thiolate complexes and salts [36, 37], and formation of $Bi(CyS)_3$ on Bi electrodes [38].

The cysteine determination was performed at pH 4.5. Although at this pH a dissociation degree of thiol group will be decreased, this pH can prevent the formation of Bi hydroxide species at the electrode surface. Also, as a consequence of the formation of Bi hydroxide species, yield of the Bi-cysteinate will be decreased.

For accumulation of bismuth(III) cysteinate the potential of -0.4 V was chosen, as this potential ensures formation of bismuth(III) cysteinate at electrodes surface and in the same time avoids active dissolution of Bi which may distort adsorbed $Bi(Cys)_3$ layer.

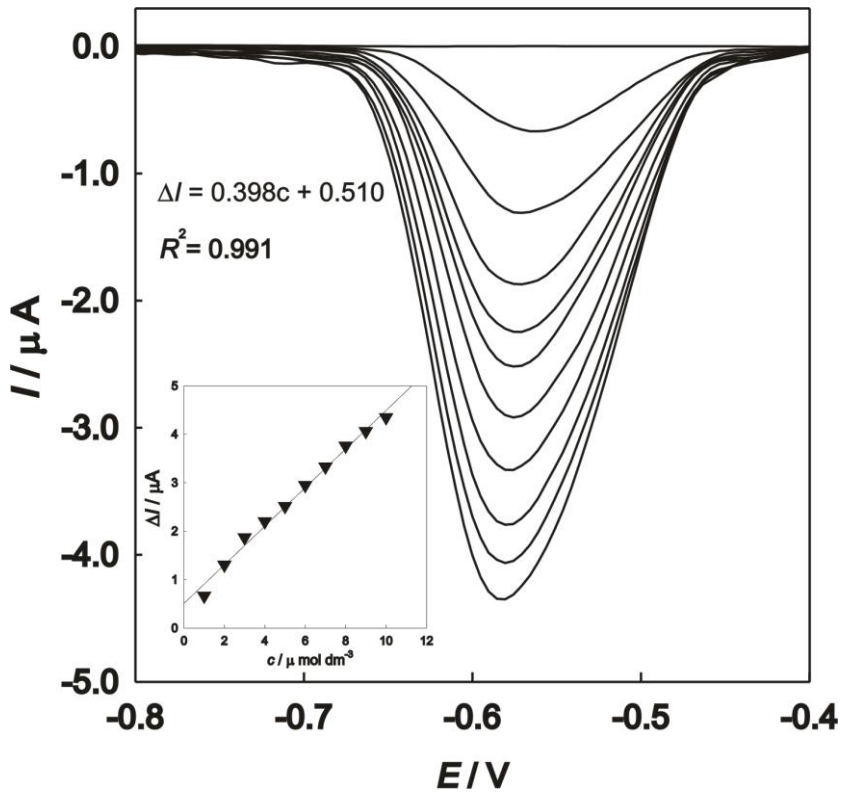

Figure 6. SWCSVs with baseline correction, recorded at Bi-film/CFME in acetate buffer solution (pH 4.5) with successive addition of cysteine in 1.0 μmol dm^{-3} steps from 1.0 μmol dm^{-3} to 10.0 μmol dm^{-3} together with background response. Experimental conditions: accumulation potential − 0.4 V, accumulation time 540 s, equilibration time 60 s, frequency 10 Hz, pulse amplitude 50 mV and scan increment 5 mV. The inset shows the corresponding calibration plot.

From monitoring the influence of applied potential increment (ΔE_s), frequency (f) and pulse height (ΔE_p) on reduction peak currents (I_p), optimal SWCSV procedure has been established: f = 50 Hz, ΔE_s = 5 mV and ΔE_p = 50 mV.

The results of SWCSV in the presence of different cysteine concentration are shown in Fig. 6, with corresponding calibration graphs as insets. The voltammograms were obtained by standard addition method at Bi-film/CFME and presented curves are background-subtracted reduction currents. In the concentrations range between 1.0 μmol dm^{-3} and 10.0 μmol dm^{-3} of cysteine, the calculated detection limit, based on the 3σ criterion [34], was 0.028 μmol dm^{-3}, with the sensitivity of 398 nA μmol^{-1} dm^{-3}. Compared to the previously studies, reported for modified carbon materials, this method exhibited remarkable analytical performances (high sensitivity, low detection limit and broad linear range).

In order to evaluate the analytical applicability of the proposed method, it was successfully applied for the detection of N-acetyl cysteine (NAC) in NAC-Twinlab® dietary supplement and results are given in Table 1. The concentrations of NAC were obtained using the standard addition method. Recoveries of 97.5% to 100.1% from food supplement suggest that this method is very reliable and sensitive.

Table 1. The application of BiF-RACFMEs for determination of NAC (n = 3) in NAC-Twinlab® dietary supplement.

Sample No.		1	2	3	4	5
Original content	μmol dm^{-3}	1	1	1	1	1
Added	μmol dm^{-3}	-	2	4	6	8
Peak current	μA	0.67	1.16	1.65	2.19	2.69
Found	μmol dm^{-3}	-	2.95	4.93	7.03	9.01
Recovery	%	-	97.5	99.0	100.5	100.1

4. CONCLUSION

Cyclic voltammetry and chronoamperometric studies have been carried out for bismuth electrodeposition, from 0.5 mol dm^{-3} HNO_3, on different carbon based materials. Deposition process is limited by Bi^{3+} diffusion from the bulk solution. Using Randles-Sevcik equation, calculated values of Bi^{3+} diffusion coefficients from measurements with GCE and GPE were 5.8×10^{-6} cm^2 s^{-1} and 7.3×10^{-6} cm^2 s^{-1}, respectively. From measurements with CFME Bi^{3+} diffusion coefficient was obtained by using equation for the case when no more overlapping of the individual diffusion is noticed and it was 1.4×10^{-6} cm^2 s^{-1}. In the case of the CFME and GPE, analysis of current-time transients, using Scharifker-Hills models, has shown that mechanism of nucleation is shifted from 3D progressive to 3D

instantaneous with increasing Bi^{3+} concentration. For CFME, throughout all measured concentration range, instantaneous nucleation was observed.

The ex-situ formed bismuth film on CFME has been applied in electroanalytical determination of cysteine by SWCSV. The detection limit of 0.028 μmol dm^{-3} with sensitivity of 398 nA μmol^{-1} dm^{-3} was obtained in concentration range between 1.0 μmol dm^{-3} and 10.0 μmol dm^{-3}.

References

1. H. P. Chang, D. C. Johnson, *Anal. Chim. Acta*, 248 (1991) 85
2. S. Legeai, S. Bois, O. Vittori, *J. Electroanal.Chem.*, 591 (2006) 93
3. I. Svancara, K. Vytras, *Chem. Listy*, 100 (2006) 90
4. N. Yu. Stozhko, N.A. Malakhova, M.V. Fyodorov, K.Z. Brainina, *J. Solid State Electrochem*,. 12 (2008) 1185
5. N. Yu. Stozhko, N.A. Malakhova, M.V. Fyodorov, K.Z. Brainina, *J. Solid State Electrochem.*, 12 (2008) 1219
6. A. Economou, *Trends in Anal. Chem.*, 4 (2005) 334
7. I. Svancara, C. Prior, S. B. Hocevar, J. Wang, *Electroanalysis*, 22 (2010) 1405
8. J. Wang, *Electroanalysis*, 17 (2005) 1341
9. Z. D. Anastasiadou, I. Sipaki, P. D. Jannakoudakis , S. T. Girousi, *Anal. Letters*, 44 (2011) 761
10. F. Arduini, J. Q. Calvo, A. Amine, G. Palleschi, D. Moscone, *Trends in Anal. Chem.*, 29 (2010) 1295
11. J. Wang, J. Lu, S. B. Hocevar, P. A.M. Farias, *Anal. Chem*., 72 (2000) 3218
12. O. Ordeig, J. del Campo, F. X. Munoz, C. E.Banks, R. G. Compton, *Electroanalysis*, 19 (2007) 1973
13. S. Fletcher, M. D. Horne, *Electrochem. Commun.*, 1 (1999) 502
14. B. R. Scharifker, G. Hills, *Electrochim. Acta*, 28 (1983) 879
15. Z. Grubač, M. Metikoš-Huković, *Mater. Lett.*, 61 (2007) 794
16. Z. Petrović, M. Metikos-Hukovic, Z. Grubac, S. Omanovic, *Thin Solid Films*, 513 (2006) 193
17. K. Winkler, *J. Electroanal. Chem.*, 388 (1995) 151
18. A. Dekanski, J. Stevanovic, R. Stevanovic, B. Z. Nikolic, V. M. Jovanovic, *Carbon*, 39 (2001) 1195
19. E. Sandnes, M. E. Williams, U. Bertoci, M. D. Vaudin, G. R. Stafford, *Electrochim. Acta*, 52 (2007) 6221
20. M. Yang, Z. Hu, *J. Electroanal. Chem.*, 583 (2005) 46
21. A. Krolicka, A. Bobrowski, *Electrochem. Commun*., 6 (2004) 99
22. D. Grujičić, B. Pesić, *Electrochim. Acta*, 47 (2002) 2901
23. L. Heerman, A. Tarallo, *J. Electroanal. Chem*., 451 (1998) 101
24. T. J. Davies, R. G. Compton, *J. Electroanal. Chem*., 585 (2005) 63
25. A. J. Bard, L. R. Faulkner, Electrochem. Methods: Fundamentals and Applications, New York (2001)
26. L. Heerman, A. Tarallo, *Electrochem. Commun.*, 2 (2000) 85
27. J. Mostany, J. Mozota, B. R. Scharifker, *J. Electroanal. Chem.*, 29 (1984) 25
28. M. P. Pardave, M. T. Ramirez, I. Gonzales, A. Serruya, B. R. Scharifker, *J. Electrochem. Soc*., 143 (1996) 1551
29. D. Grujicic, B. Pesic, *Electrochim. Acta*, 49 (2004) 4719
30. M. L. S. Simoes Goncalves, M. M. Correia Dos Santos, *J. Electroanal. Chem.*, 163 (1984) 315
31. J. W. Fitzerald, D. D. Hale, W. T. Swank, *Soil Biol. Biochem.*, 20 (1988) 825
32. S. Brinić, N. Vladislavić, M. Buzuk, M. Bralić, M. Solić, *J. Electroanal. Chem.*, 705 (2013) 86

33. L. Baldrianova, P. Agrafiotou, I. Svancara, K. Vytras, S. Sotiropoulos, *Electrochem. Commun.*, 10 (2008) 918
34. S. Cakir, E. Bicer, O. Cakir, *Electrochem. Commun.*, 1 (1999) 257
35. B. Monterroso-Marco, B. Lopez-Ruiz, *Talanta*, 61 (2003) 733
36. N. Burford, M.D. Eelman, D.E. Mahony, M. Morash, *Chem. Commun.*, 1 (2003) 146
37. H.A. Phillips, M.D. Eelman, N. Burford, *J. Inorg. Biochem.*, 101 (2007) 736
38. T. Romann, V. Grozovski, E. Lust, *Electrochem. Commun.*, 9 (2007) 2507
39. J. Mocak, A. M. Bond, S. Mitchell, G. Scollary, *Pure & Appl. Chem.*, 69 (1997) 297